# Basic considerations on spectral coherent combining for high combining performance

Yaqi Wu<sup>1</sup>, Bowen Liu<sup>1,2</sup>, Genyu Bi<sup>1</sup>, Chenming Yu<sup>1</sup>, and Minglie Hu<sup>1,2</sup>

<sup>1</sup> Ultrafast Laser Laboratory, Key Laboratory of Opto-Electronic Information Science and Technology of Ministry of Education, School of Precision Instruments and Opto-Electronics Engineering, Tianjin University, Tianjin 300072, China

<sup>2</sup> Georgia Tech Shenzhen Institute, Tianjin University, Shenzhen 518071, Guangdong Province,

#### China

Abstract Spectral coherent combining (SCC) offers a powerful approach to increase output power and shorten pulse duration. Here, we comprehensively investigate SCC of two beams to achieve the high combining performance. The preliminary analysis indicates incident spectra and the transition region of the combiner both affect the combining process. The simulation results show that optimizing the overlapping spectral range, the transition width and start wavelength of the combiner can achieve the high combining efficiency and high pulse quality. Guided by the

Correspondence to: Bowen Liu, Ultrafast Laser Laboratory, Key Laboratory of Opto-Electronic Information Science and Technology of Ministry of Education, School of Precision Instruments and Opto-Electronics Engineering, Tianjin University, Tianjin 300072, China. Email: bwliu@tju.edu.cn

This peer-reviewed article has been accepted for publication but not yet copyedited or typeset, and so may be subject to change during the production process. The article is considered published and may be cited using its DOI.

This is an Open Access article, distributed under the terms of the Creative Commons Attribution licence (https://creativecommons.org/licenses/by/4.0/), which permits unrestricted re-use, distribution, and reproduction in any medium, provided the original work is properly cited.

10.1017/hpl.2025.10082

simulation results, we built a femtosecond laser system based on SCC of two fiber amplifiers,

achieving 96.9% combining efficiency and high-quality 42-fs pulses. To the best of our

knowledge, this is the first time that the high combining efficiency and high pulse quality are

achieved simultaneously in a fiber femtosecond laser system based on SCC. This study provides

design guidelines for the high-performance combination of beams covering different spectral

regions.

Key words: femtosecond laser; spectral coherent combining; fiber amplifiers

I. INTRODUCTION

Femtosecond fiber lasers are highly demanded due to the good beam quality, high stability, low

cost and compactness. They have been utilized to generate high-harmonics and terahertz

radiation [1,2]. However, the long propagation length and the limited core diameter intensify the

nonlinear effects and distort the pulse quality, hindering the scaling of the system performance.

To alleviate nonlinearity, chirped pulse amplification (CPA) is widely adopted to improve the

output energy. At present, the femtosecond fiber laser system can output 2.2-mJ pulse energy,

but output energy is limited by the damage threshold [3]. Furthermore, thermal problem cannot be

neglected when fiber lasers work in high-power operation. The onset of transverse mode

instability distorts the beam quality and limits the scaling of average power [4]. In the past

decade, coherent beam combination has demonstrated its unique ability to solve these problems,

multiplying the output power and energy [5,6]. In addition to pulse energy and average power,

pulse duration is also demanded for some applications. Although the Yb-doped fiber has a broad

gain spectrum, the output pulse duration of high energy fiber amplifiers almost > 200 fs due to

the gain narrowing effect [7,8]. To generate shorter pulse duration, some ways have been proposed

to broaden the output spectrum.

2

The simplest method is spectral shaping, which pre-attenuates spectral components around gain peak. It usually places spectral notch filters before the amplifier to shape the spectrum and has been demonstrated to deliver 55-fs pulses in a fiber CPA system with low pulse energy <sup>[9]</sup>. However, notch filters have fix parameters and only supply a weak attenuation, which is not suitable for high-gain fiber CPA systems. Spatial light modulator is a powerful tool to flexibly tailor the spectrum and can supply strong attenuation, it has been used to achieve 130-fs, 250-µJ pulses in a rod-type fiber amplifier and 120-fs, 10-mJ pulses in a coherently combined fiber CPA system <sup>[10,11]</sup>. However, the shortest pulse duration is around 100 fs in the high-energy CPA system, shorter pulse duration is difficult to achieve under the high gain.

Nonlinear pulse compression techniques, which rely on spectral broadening induced by Kerr effect and subsequent chirp compensation, have been developed to generate few-cycle pulses [12–14]. However, such systems require a long optical arrangement, and the nonlinear effect induces the modulated spectrum, resulting in pulse pedestals [15].

In recent years, coherent combining several channels with different spectral regions has been demonstrated to generate shorter pulses. Spectral coherent combining (SCC) was firstly widely used to achieve few-cycle or even sub-cycle pulses, and then extent to the Yb-doped fiber amplification system to overcome the gain narrowing effect <sup>[16,17]</sup>. Combining several fiber amplifiers with different spectra was firstly demonstrated in 2013, and using it to generate a broadener spectrum compared with a single amplifier under the same high gain <sup>[18,19]</sup>. Then, 97-fs pulse duration and 10-μJ pulse energy were achieved from a two-channels fiber amplification system based on SCC with the high-order dispersion compensation <sup>[20]</sup>. Moreover, combining the spectral shaping and high-order dispersion compensation, a three channels fiber amplification system based on SCC can generate 42-fs pulses, but the average power is low and the pulse

shows obvious pedestals <sup>[21]</sup>. Table 1 summaries experimental results of Yb-doped fiber amplification systems based on SCC. Normally, the combining efficiency is less than 90% for most fiber amplification systems based on SCC and the combining efficiency can be improved by decreasing the overlapping spectral range, but this greatly degrades the pulse quality. Therefore, it is necessary to analyze the combining process and study how to improve the combining performance to achieve the high combining efficiency and high pulse quality.

Table 1. Overview of Yb-doped fiber amplification systems based on SCC

Pulse duration (fs)	Average power (W)	Repetition frequency (MHz)	Combining efficiency (%)	Reference
403	0.26	72	76.3	[18]
356	0.27	72	85.8	[18]
130	6	35	86	[19]
97	10	1	89	[20]
42	\	100	93.6	[21]
42	23	49	96.9	this work

In this paper, we investigate SCC of two beams to achieve the high combining performance. Firstly, we analyze the combining process and find that incident spectra and the transition region of the combiner both affect the combining performance. Then the numerical simulation indicates more overlapping spectra can improve the combined pulse quality while sacrificing the combined pulse duration. On the other hand, the combining performance can be improved by optimizing the start wavelength (SW) and transition width (TW) of the combiner. Moreover, a few overlapping spectra relax the strict requirement for the TW and SW of the combiner and can easily achieve a high combining efficiency. Besides, the spectral phase mismatch also affects the combining process, but SCC is less sensitive to the spectral phase difference than the filled-aperture combining. According these simulation results, we built a

femtosecond laser system based on SCC of two fiber amplifiers, achieving the 96.9% combining efficiency and generating high-quality 42-fs pulses. To the best of our knowledge, this is the first time that the high combining efficiency and high pulse quality are achieved simultaneously in a fiber femtosecond laser system based on SCC. This work provides design guidelines for the high-performance combination of beams covering different spectral regions.

# **II. NUMERICAL SIMULATION**

In spectral coherent combining, the dichroic mirror (DM) is always used as the combiner and plays an important role in the combining process. The combining efficiency, as well as spectrum and pulse quality of the combined beam, are all related to the transmittance curve of the DM. Taking the longpass dichroic mirror (LP-DM) as an example, as shown in Fig. 1, a polyline represents the typical transmittance curve of the LP-DM (purple dashed line) and a transition region exists on the transmittance curve of the LP-DM (gray shaded area), which cannot be very sharp due to the limitation of coating technology. The  $\lambda_1$  and  $\lambda_2$  represent edge wavelengths of the transition region. The  $\lambda_1$  and  $\lambda_2$ - $\lambda_1$  are referred to as the SW and TW, respectively. In the combining process, the spectra of the transmitted and reflected beams are on both sides of the transmittance curve, with some overlapping spectra in the transition region (Fig. 1). It's obvious that the transition region greatly affects the combining performance, but it has not been analyzed in detail. In this section, we concentrate on the combining process, and numerically investigate the influences of incident spectra and the transition region of the combiner on this process.

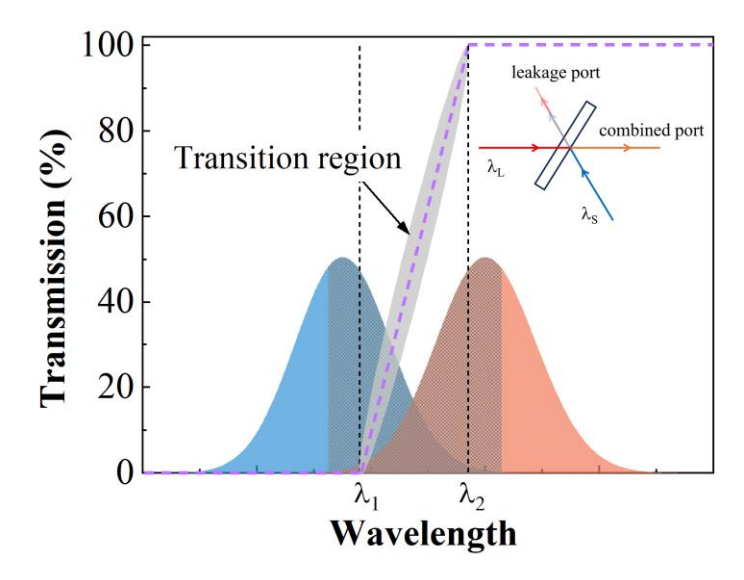


Fig. 1. The typical transmittance curve of the LP-DM (purple dashed line), spectra of incident beams (shaded area) and their overlapping part (grid area). The  $\lambda_1$  and  $\lambda_2$ - $\lambda_1$  are referred to as the SW and TW, respectively. The inset shows the combining process.

For SCC, when the LP-DM as a combiner, two beams with long-wavelength  $\lambda_L$  and short-wavelength  $\lambda_S$  combine into a beam with a wide spectrum (Fig. 1 inset), and the in-phase combining efficiency for each spectral component is

$$\eta(\lambda) = \frac{P_{com}(\lambda)}{P_{S}(\lambda) + P_{L}(\lambda)} = \frac{\left[\sqrt{P_{L}(\lambda) \cdot T(\lambda)} + \sqrt{P_{S}(\lambda) \cdot (1 - T(\lambda))}\right]^{2}}{P_{S}(\lambda) + P_{L}(\lambda)} \tag{1}$$

where  $P_S$  and  $P_L$  are spectral power of two beams, T is the transmittance of the combiner. Only when the incident power ratio equals to the splitting ratio  $(P_S(\lambda)/P_L(\lambda)=(1-T(\lambda))/T(\lambda))$ , it can achieve a perfect combination [22]. In other words, matching spectral intensity of each channel to splitting ratios of the combiner at each wavelength can achieve the highest combining efficiency. Thus, spectra of incident beams and the transition region of the combiner both affect the combining process. In the following, we numerically simulate SCC of two beams with identical

energy under in-phase to investigate influences of incident spectra and the transition region of the combiner on the combining process.

# 2.1 Influence of incident spectra

Firstly, the influence of the interval between central wavelengths of beams on combined pulses is investigated. Two pulses are 80-fs transform-limited (TL) Gaussian pulses. The central wavelength of the long-wavelength channel (CW-LWC) is 1060 nm, and the central wavelength of the short-wavelength channel (CW-SWC) gradually red-shifts from 1020 nm to 1040 nm. They are combined by a DM with 20-nm TW and 1038-nm SW and results are shown in Fig. 2. As the CW-SWC blue-shifts, the overlapping spectral range decreases, leading to the broadened spectrum with a deep and wide gap (Fig. 2(a)). As a result, the combined pulse shows a shorter pulse duration, accompanied by the presence of side lobes (Fig. 2(b). This also reduces the energy ratio of the main peak over the whole pulse [23] (Fig. 2(c)). Overall, less overlapping spectra can combine a shorter pulse duration while sacrificing the pulse quality for fixed incident pulse durations, so there should be a tradeoff between the pulse duration and pulse quality.

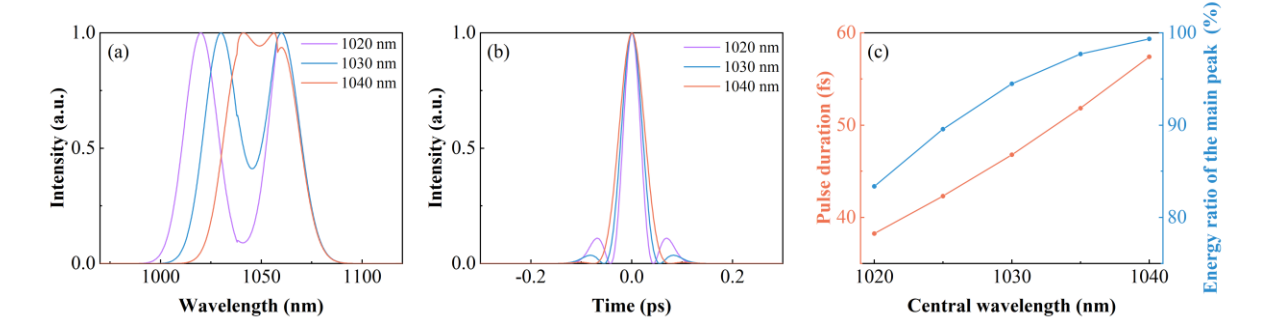


Fig.2. The combined spectra (a) and pulses (b) under different CWs-SWC. (c) The energy ratio of the main peak and pulse duration of the combined pulse versus the CW-SWC.

Then, the influence of spectral bandwidths of two beams on combined pulses is investigated. Two pulses are TL Gaussian pulses, centered at 1035 nm and 1060 nm respectively, and they are combined by a DM with 20-nm TW and 1038-nm SW. When the spectral bandwidth increases, the corresponding pulse duration decreases. Therefore, we change the incident pulse duration to represent the change of spectral bandwidth. As incident pulses gradually shorten from 100 fs to 40 fs, the combined spectrum broadens and the gap disappears (Fig. 3(a)). As a result, the combined pulse shows a shorter pulse duration and higher energy ratio of the main peak (Fig. 3(c)). However, the combined pulse does not significantly shorten compared with incident pulses. For example, two 100-fs pulses can combine a 57-fs pulse, but the combination of two 40-fs pulses only can generate a 33-fs pulse. This indicates that the advantage of SCC gradually weakens as incident pulses shorten. To illustrate this phenomenon, the spectral broadening ratio is introduced, which is equal to the combined spectral bandwidth divided by the incident spectral bandwidth. As the incident pulse shortens, the overlapping spectral range gradually increases, which decreases the spectral broadening ratio, so the combined pulse duration becomes short slightly (Fig. 3(b)). Overall, more overlapping spectra can improve the combined pulse quality while sacrificing the pulse duration.

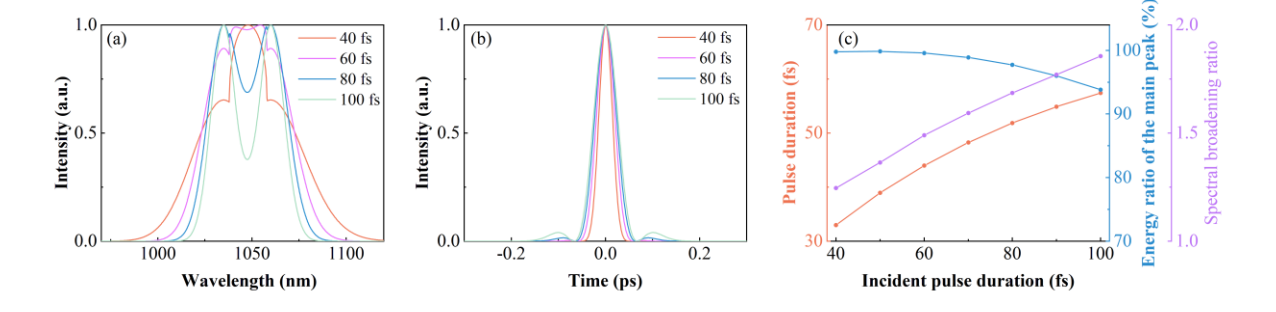


Fig. 3. The combined spectra (a) and pulses (b) under different incident pulse durations. (c) The energy ratio of main peak, pulse duration and spectral broadening ratio of combined pulses versus the incident pulse duration.

# 2.2 Influence of the transition region of the combiner

Next, the influence of the SW of the combiner on the combining process is investigated. Two pulses are 80-fs TL Gaussian pulses, centered at 1035 nm and 1060 nm respectively and combined by a DM with 19-nm TW and different SWs. As shown in Fig. 4(a), the SW greatly affects the combining efficiency and there exists an optimal value (1038 nm) to achieve the highest combining efficiency. To illustrate this phenomenon, transmittance curves of combiners with 1030-nm and 1038-nm SW, as well as corresponding uncombined spectra of the leakage port are shown in Fig. 4(c) and (d) respectively. When the SW deviates from 1038 nm, the power of non-overlapping spectra of the leakage port (Fig. 4(c) grid area) increases. On the other hand, spectral powers of two beams in the overlapping region are significantly different at the leakage port, so they can't completely destructive interference. Those can be attributed to the mismatch between incident spectra and transmittance curve of the combiner, so results in a decline in the combining efficiency. Besides, the RMS width of the combined pulse increases with the SW deviates the optimal value (Fig. 4(a)), indicating the pulse quality gradually degrades. As the SW deviates from the optimal value, the power ratio of long-wavelength components over the combined spectrum decreases, this induces asymmetry and the significant gap of spectra (Fig. 4(a) inset), so resulting in the decreasing pulse quality.

Then, the influence of the TW is investigated, as shown in Fig. 4(b). For every TW, the SW is chosen to achieve the highest combining efficiency. Though there exists an optimal TW to achieve the highest combining efficiency, the combining efficiency is always larger than 98% when the TW changes from 11 nm to 28 nm. And the pulse quality slightly degrades under the narrow TW due to the gap of spectra (Fig. 4(b) inset). Thus, the high combining efficiency can be achieved within a wide range of the TW of the combiner. Overall, the SW and TW should be

carefully adjusted to achieve the high combining efficiency and high pulse quality, and the SW is more important for the combining process.

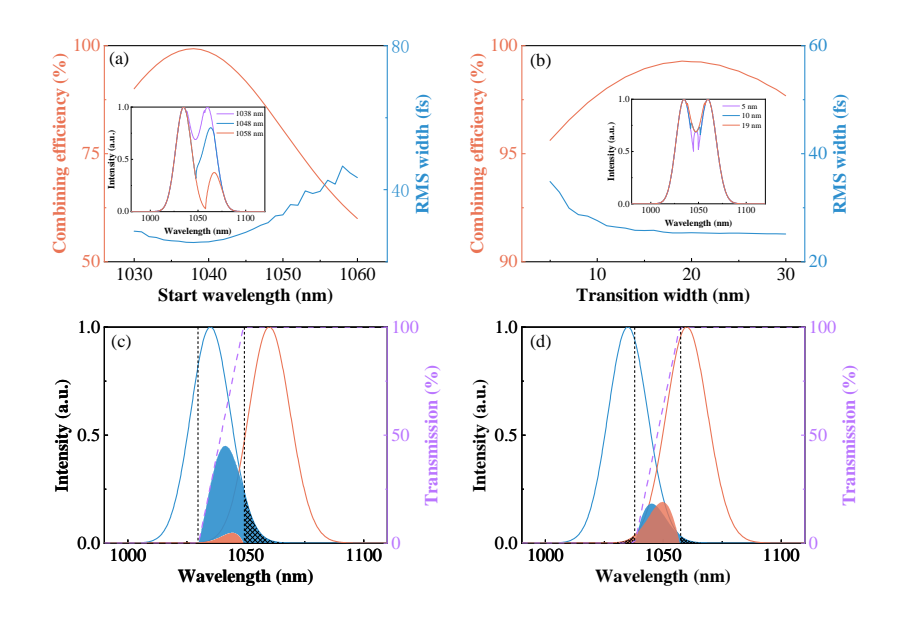


Fig. 4. (a) The combining efficiency and RMS width of the combined pulse versus the SW under 19-nm TW. The inset shows combined spectra under different SWs. (b) The combining efficiency and RMS width of the combined pulse versus the TW. The inset shows combined spectra under different TWs. (c) Incident spectra (solid lines), uncombined spectra of the leakage port (shaded area), non-overlapping spectra of the leakage port (grid area) and the transmittance curve of the combiner (purple dashed line) under 19-nm TW and 1030-nm SW. (d) Incident spectra (solid lines), uncombined spectra of the leakage port (shaded area), non-overlapping spectra of the leakage port (grid area) and the transmittance curve of the combiner (purple dashed line) under 19 nm-TW and 1038-nm SW.

For further discussion and comparison, influences of the TW and SW is investigated under different CWs-SWC. Two pulses are 80-fs TL Gaussian pulses, and the CW-LWC is fixed at 1060 nm. Fig. 5(a)-(d) show the combining efficiency versus the TW and SW when the CW-SWC is 1010 nm, 1020 nm, 1030 nm and 1040 nm respectively. It can be seen that the region for the combining efficiency >99% (encircled by the white dashed line) becomes narrower when the

CW-SWC red-shifts. As the CW-SWC red-shifts, the overlapping spectral range increases (Fig. 5(e)), the power ratio of overlapping spectra over the whole spectrum also increases. Thus, the mismatch between incident spectra and the transmittance curve of the combiner plays a greater influence on the combining efficiency, resulting in the region for the combining efficiency >99% reduces. This also leads to the highest combining efficiency decreases with the CW-SWC red-shifts (Fig. 5(f)). Besides, as the CW-SWC red-shifts, the TW needs to be increased to match the increase of overlapping spectral range in order to achieve the highest combining efficiency, as shown in Fig. 5(f).

Though the highest combining efficiency can only be achieved by the combiner with a narrow TW for a few overlapping spectra, the combiner with a wide TW can also achieve high combining efficiency. For example, as shown in Fig. 5(a), the highest combining efficiency is nearly 100% under the optimal TW (9 nm), the combiner with 20-nm TW can also achieve 99.8% combining efficiency. This can alleviate the severe demand for the high-cost DM with a sharp transition region.

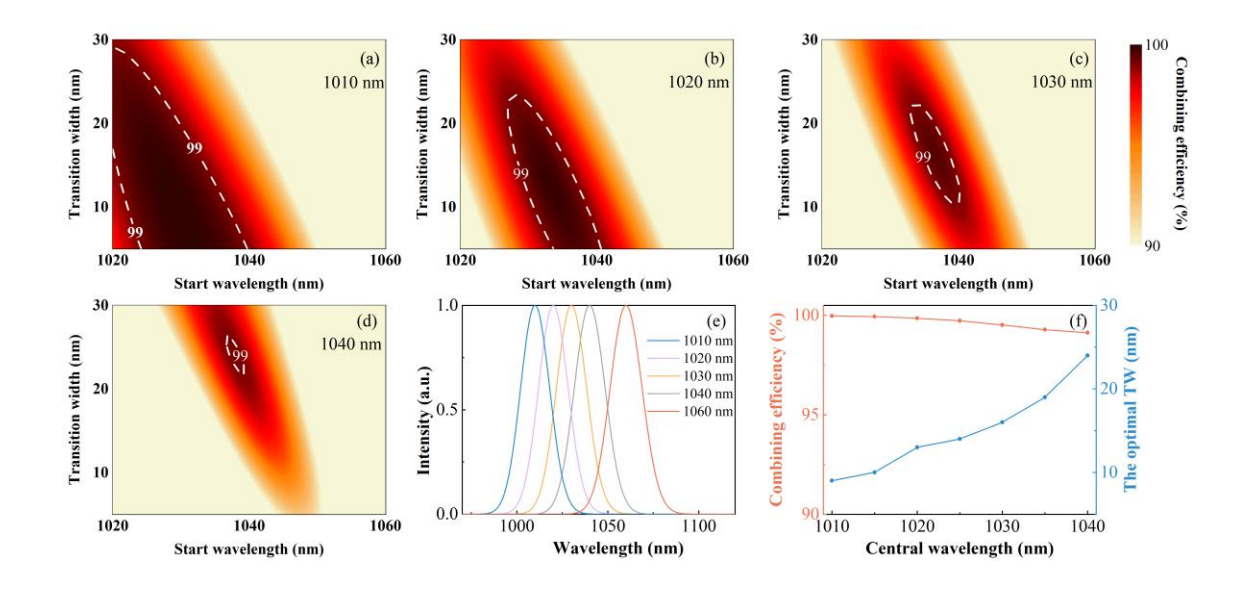


Fig. 5. Combining efficiency versus the TW and SW under the CW-SWC is (a) 1010 nm, (b) 1020 nm, (c) 1030 nm, (d) 1040 nm. (e) The incident spectra under different CWs-SWC. (f) The highest combining efficiency and the optimal TW versus the CW-SWC.

# 2.3 Influence of the spectral phase mismatch

The above results and analysis only consider the in-phase combination of TL pulses. However, the spectral phase mismatch between beams will affect the combining process and should be investigated. We simulate the combination of two 80-fs TL Gaussian pulses centered at 1035 nm and 1060 nm respectively, combined by a DM with 19-nm TW and 1038-nm SW. And one pulse is applied with the extra zero-order phase  $\varphi_0$ , delay  $\varphi_1$ , group delay dispersion  $\varphi_2$  and third-order dispersion  $\varphi_3$  respectively and results are shown as Fig. 6(a)-(d). The mismatch of the zero-order phase slightly affects the combining process. The precise matching for the delay is not necessary, a <20 fs delay (25% pulse duration) almost doesn't affect the combining process. Besides, a 2000 fs<sup>2</sup>  $\Delta \varphi_2$  and  $2 \times 10^5$  fs<sup>3</sup>  $\Delta \varphi_3$  only cause a change in the combining efficiency and pulse duration of less than 2% and 4 fs, respectively, indicating the combination is almost not affected by the mismatched  $\varphi_2$  and  $\varphi_3$ . At the same time, the RMS width slowly increases with the  $\Delta \varphi_2$  and  $\Delta \varphi_3$ , indicating the pulse quality slowly degrades, but the combined pulse still maintains a high pulse quality.

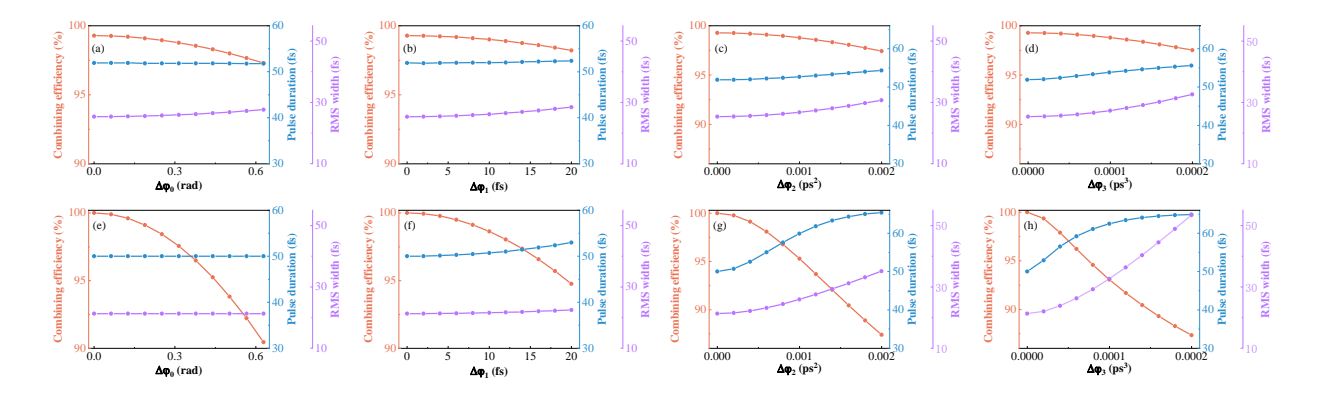


Fig. 6. (a)-(d) The combining efficiency, pulse duration and RMS width of the combined beam by SCC versus the spectral phase mismatch. (e)-(h) The combining efficiency, pulse duration and RMS width of the combined beam by the filled-aperture combining versus the spectral phase mismatch.

For comparison, the influence of spectral phase mismatch on two-channels filled-aperture combining with identical spectra is investigated. Two pulses are 50-fs TL Gaussian pulses centered at 1040 nm with same energy and combined by a 50:50 BS, one pulse is applied with the extra spectral phase. The combining efficiency is more sensitive for the mismatched zero-order phase and delay compared to the SCC, as shown in Fig. 6(e)-(h). Moreover, the combining efficiency, pulse duration and RMS width are greatly affected by the  $\Delta \phi_2$  and  $\Delta \phi_3$ . We can conclude that SCC is not sensitive to the spectral phase mismatch between beams, but the spectral phase mismatch is essential to the filled-aperture combining, which makes the control technique more difficult and complex. Thus, SCC is preferred to overcome the influence of the spectral phase mismatch between beams and achieve the nearly perfect combining process.

Now, we have performed the simulation about influences of incident spectra and the transition region of the combiner on the combining process. To achieve the high combining efficiency and high pulse quality, some overlapping spectra must exist between beams and optimizing the SW and TW of the combiner is necessary. Additionally, spectral phase mismatch should be minimized.

#### III. EXPERIMENT AND RESULTS

Based on the numerical simulation above, we built a two-channels SCC system. The experimental setup is shown as Fig. 7. The laser source is a 49 MHz femtosecond fiber laser with a Yb-doped fiber oscillator and two-stage pre-amplifiers that employs the nonlinear amplification technology to generate a broadband spectrum (inset of Fig. 7) [24]. Then output

beam is split into two channels by a LP-DM and the reflected beam passes a piezo-driven mirror located on a translation stage to compensate the phase noise and match the optical path length. In each channel, a 1000 lines/mm transmission grating pair and 6-nm bandpass filter are used to adjust the pre-chirp and central wavelength to optimize the pulse evolution in the main amplifier. The main amplifiers are two different Yb-doped tapered double-cladding fibers, counter-pumped by a laser diode (976 nm). The gain fiber 1 has a monotone increasing core and cladding diameters along the 1.8-m fiber with 25 dB/m pump absorption at 976 nm and core diameters are about 9 µm and 40 µm respectively on the thin and wide sides. The gain fiber 2 only has a 0.7-m taper region at middle part with 8 dB/m pump absorption at 976 nm and the core diameters are 35 µm and 56 µm respectively on the 1.2-m thin and 0.5-m wide sides. After amplified, the output pulses are compressed by a 1000 lines/mm transmission grating pair. Then compressed pulses with different spectra are combined by a LP-DM and a little part of combined beam is directed to the photodiode for active phase stabilization by a 1:99 beam splitter, the main part is sent into the power meter. The stable constructive superposition is performed by the singledetector electronic frequency-tagging (LOCSET), a beam is used as the reference and another is imprinted by the 9 kHz tagging frequency [25]. The system control demodulates the error signal and applies it to the piezo-driven mirror to achieve the close loop.

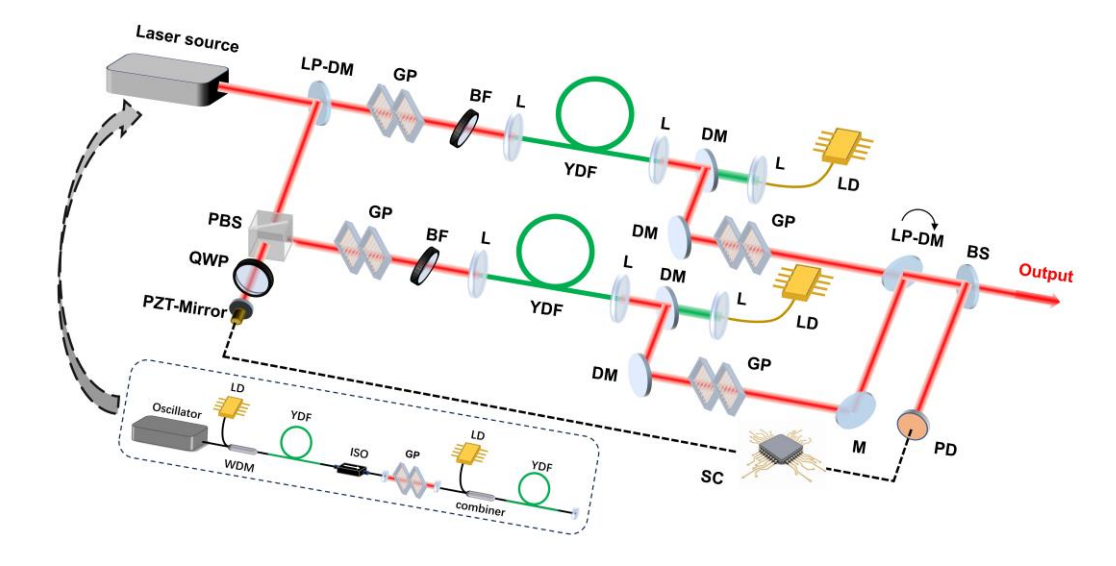


Fig. 7. Schematic of the experimental setup. WDM: wavelength division multiplexer; ISO: isolator; LP-DM: long-pass dichroic mirror; HWP: half-wave plate; QWP: quarter-wave plate; PBS: polarizing beam splitter; PZT-Mirror: piezo-driven mirror; GP: grating pair; BF: bandpass filter; YDF: Yb-doped fiber; L: lens; DM: dichroic mirror; M: mirror; BS: beam splitter; PD: photodiode; LD: laser diode; SC: system control. The inset shows the schematic of the laser source.

In the experiment, the input energy and initial chirp are adjusted to achieve the nearly TL amplified pulse after compression under the fixed pump power for two channels. The output average powers are 12.4 W and 11.4 W respectively, and corresponding nonlinear phases are  $8\pi$  and  $6\pi$ . The output spectra are shown in Fig. 8(a), there is an overlapping spectral region of 1042-1060 nm to ensure the phase locking and achieve the high pulse quality of the combined beam. The autocorrelation (AC) traces of dechirped pulses of two channels are shown in Fig. 8(b), the pulse durations are 70 fs and 73 fs respectively, close to TL duration 68 fs. In the combination, the combination efficiency and combined pulse duration are both sensitive to the delay. Unfortunately, they cannot achieve optimal results simultaneously by changing the delay. The highest combining efficiency is 97.3%, but it decreases to 96.8% when the delay is tuned to zero to obtain the shortest the AC duration, as shown in Fig. 8(c). This behavior can be

understood as the delay can partially compensate the phase difference, but the induced delay will affect the combined pulse. In fact, the combining efficiency is related to the phase difference of two beams, and the AC duration of the combined beam is related to the temporally overlap of two pulses. Therefore, the induced delay compensating the spectral phase difference causes the separation of the two pulses, resulting in the higher combining efficiency and longer pulse duration. In the experiment, the delay should be adjusted to achieve the shortest pulse duration, because SCC is proposed to generate a short pulse duration.

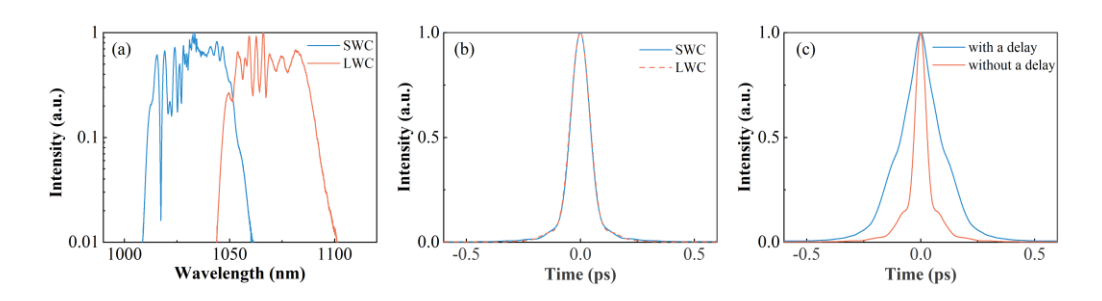


Fig. 8. (a) The output spectra and (b) AC traces of two channels. (c) The AC traces of the combined beam with different delays.

As mentioned in the numerical simulation, the SW of the combiner can greatly influence the combining efficiency. Thus, we change the SW of the combiner by tuning the incident angle of beam to the combiner in order to improve the combining efficiency, results are shown in Fig. 9(a). The highest combining efficiency is 96.8% and the corresponding combined pulse duration is 42 fs, but the pulse quality is not high (Fig. 9(c) blue line). According to previous results, the appropriate TW may improve the combining performance, so another LP-DM with a wide TW (20 nm) is employed to optimize the combination, as shown in Fig. 9(b). The highest combining efficiency is 96.9%, the corresponding combined pulse duration is 42 fs and the pulse quality is significantly improved (Fig. 9(c) red line). Thus, it is demonstrated that the high combining

efficiency and high-quality pulses can be obtained by optimizing the SW and choosing the appropriate TW of the DM.

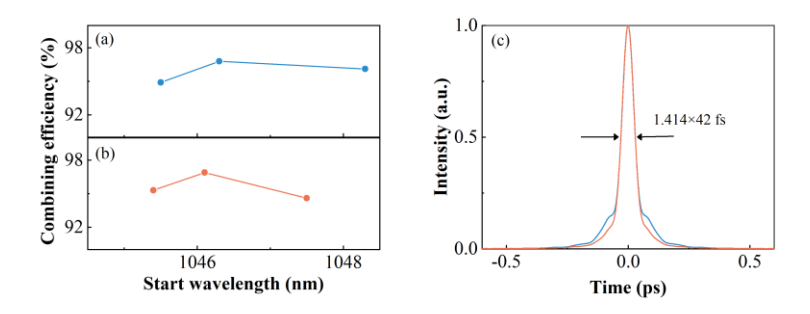


Fig. 9. The combining efficiency versus the SW of the combiner with a (a) narrow (12 nm) and (b) wide (20 nm) TW. (c) The AC traces of combined pulses with a narrow (blue) and wide (red) TW under the highest combining efficiency.

#### IV. CONCLUSION

In conclusion, the SCC system employing the DM as a combiner is investigated in detail. The preliminary analysis indicates incident spectra and the transition region of the combiner both affect the combining process, and the highest combining efficiency can be achieved when the spectral intensity of each channel matches the splitting ratio of the combiner at each wavelength. Then the numerical simulation is performed to investigate influences of incident spectra and the transition region of the combiner on the combined pulse and combining efficiency. The simulation results show more overlapping spectra can improve the combined pulse quality while sacrificing the pulse duration. Moreover, the TW and SW both affect the combining efficiency and combined pulse quality, and they should be optimized to achieve the high combining performance. Besides, a few overlapping spectra of beams relax the strict requirement for the TW and SW of the combiner and easily achieve a high combining efficiency. On the other hand, the spectral phase mismatch also affects the combining process, but SCC is less sensitive to the spectral phase difference than the filled-aperture combining. Guided by the above results, an

experiment is designed to achieve SCC of two fiber amplifiers, and the system generates 42-fs high-quality pulse with the 96.9% combining efficiency by optimizing parameters of the combiner. This system outperforms previously demonstrated sources due to the high combining efficiency and high pulse quality.

# **Acknowledgement**

This work was supported by the National Natural Science Foundation of China (62435005) and the National Key Research and Development Program of China (2021YFB3602600).

# References

- R. Klas, A. Kirsche, M. Gebhardt, J. Buldt, H. Stark, S. Hädrich, J. Rothhardt, and J. Limpert, "Ultra-short-pulse high-average-power megahertz-repetition-rate coherent extreme-ultraviolet light source," Photonix 2, 4 (2021). DOI: https://doi.org/10.1186/s43074-021-00028-y.
- 2. J. Buldt, H. Stark, M. Muller, C. Grebing, C. Jauregui, and J. Limpert, "Gas-plasma-based generation of broadband terahertz radiation with 640 mW average power," Opt. Lett 46, 5256-5259 (2021). DOI: https://doi.org/10.1364/OL.442374.
- 3. T. Eidam, J. Rothhardt, F. Stutzki, F. Jansen, S. Hadrich, H. Carstens, C. Jauregui, J. Limpert, and A. Tunnermann, "Fiber chirped-pulse amplification system emitting 3.8 GW peak power," Opt. Express 19, 255-260 (2011). DOI: https://doi.org/10.1364/OE.19.000255.
- 4. C. Jauregui, J. Limpert, and A. Tuennermann, "High-power fibre lasers," Nature Photonics 7, 861-867 (2013). DOI: https://doi.org/10.1038/NPHOTON.2013.273.

- M. Muller, C. Aleshire, A. Klenke, E. Haddad, F. Legare, A. Tunnermann, and J. Limpert, "10.4 kW coherently combined ultrafast fiber laser," Opt. Lett 45, 3083-3086 (2020). DOI: https://doi.org/10.1364/OL.392843.
- H. Stark, M. Benner, J. Buldt, A. Klenke, and J. Limpert, "Pulses of 32 mJ and 158 fs at 20kHz repetition rate from a spatiotemporally combined fiber laser system," Opt. Lett 48, 3007-3010 (2023). DOI: https://doi.org/10.1364/OI.488617.
- M. E. V. Pedersen, M. M. Johansen, A. S. Olesen, M. Michieletto, M. Gaponenko, and M. D. Maack, "175 W average power from a single-core rod fiber-based chirped-pulse-amplification system," Opt. Lett 47, 5172-5175 (2022). DOI: https://doi.org/10.1364/OL.471631.
- 8. C. P. K. Manchee, J. Möller, and R. J. D. Miller, "Highly stable, 100 W average power from fiber-based ultrafast laser system at 1030 nm based on single-pass photonic-crystal rod amplifier," Opt. Commun 437, 6-10 (2019). DOI: https://doi.org/10.1016/j.optcom.2018.12.041.
- 9. H. Takada, Y. Chiba, D. Yoshitomi, K. Torizuka, and K. Misawa, "41-fs, 35-nJ, Green Pulse Generation from a Yb-doped Fiber Laser System," Opt. Express 25, 2115-2120 (2017). DOI: https://doi.org/10.1364/OE.25.002115.
- 10. L. Lavenu, M. Natile, F. Guichard, Y. Zaouter, M. Hanna, E. Mottay, and P. Georges, "High-energy few-cycle Yb-doped fiber amplifier source based on a single nonlinear compression stage," Opt. Express 25, 7530-7537 (2017). DOI: https://doi.org/10.1364/OE.25.007530.
- 11. H. Stark, J. Buldt, M. Muller, A. Klenke, and J. Limpert, "1 kW, 10 mJ, 120 fs coherently combined fiber CPA laser system," Opt. Lett 46, 969-972 (2021). DOI: https://doi.org/10.1364/OL.417032.

- 12. T. Nagy, S. Hädrich, P. Simon, A. Blumenstein, N. Walther, R. Klas, J. Buldt, H. Stark, S. Breitkopf, P. Jójárt, I. Seres, Z. Várallyay, T. Eidam, and J. Limpert, "Generation of three-cycle multi-millijoule laser pulses at 318 W average power," Optica 6, 1423-1424 (2019). DOI: https://doi.org/10.1364/Optica.6.001423.
- 13. M. Muller, J. Buldt, H. Stark, C. Grebing, and J. Limpert, "Multipass cell for high-power few-cycle compression," Opt. Lett 46, 2678-2681 (2021). DOI: https://doi.org/10.1364/OL.425872.
- 14. T. Okamoto, Y. Kunihashi, Y. Shinohara, H. Sanada, K. Oguri, and M. C. Chen, "Operation at 1 MHz of 1.7-cycle multiple plate compression at 35-W average output power," Opt. Lett 48, 2579-2582 (2023). DOI: https://doi.org/10.1364/Ol.477372.
- 15. E. Escoto, A. L. Viotti, S. Alisauskas, H. Tünnermann, I. Hartl, and C. M. Heyl, "Temporal quality of post-compressed pulses at large compression factors," J. Opt. Soc. Am. B 39, 1694-1702 (2022). DOI: https://doi.org/10.1364/Josab.453901.
- 16. C. Manzoni, O. D. Mücke, G. Cirmi, S. B. Fang, J. Moses, S. W. Huang, K. H. Hong, G. Cerullo, and F. X. Kärtner, "Coherent pulse synthesis: towards sub-cycle optical waveforms," Laser Photonics Rev 9, 129-171 (2015). DOI: https://doi.org/10.1002/lpor.201400181.
- 17. A. C. Ge, B. W. Liu, W. Chen, H. C. Tian, Y. J. Song, L. Chai, and M. L. Hu, "Generation of few-cycle laser pulses by coherent synthesis based on a femtosecond Yb-doped fiber laser amplification system," Chin. Opt. Lett 17(2019). DOI: https://doi.org/10.3788/Col201917.041403.
- 18. W. Z. Chang, T. Zhou, L. A. Siiman, and A. Galvanauskas, "Femtosecond pulse spectral synthesis in coherently-spectrally combined multi-channel fiber chirped pulse amplifiers," Opt. Express 21, 3897-3910 (2013). DOI: https://doi.org/10.1364/OE.21.003897.

- 19. F. Guichard, M. Hanna, L. Lombard, Y. Zaouter, C. Honninger, F. Morin, F. Druon, E. Mottay, and P. Georges, "Two-channel pulse synthesis to overcome gain narrowing in femtosecond fiber amplifiers," Opt. Lett 38, 5430-5433 (2013). DOI: https://doi.org/10.1364/OL.38.005430.
- 20. F. Guichard, M. Hanna, R. Chiche, Y. Zaouter, F. Zomer, F. Morin, C. Hönninger, E. Mottay, and P. Georges, "10μJ, ultrashort sub-100 fs FCPA synthesizer," J. Ballato, ed. (San Francisco, California, United States, 2016), p. 97282X.
- 21. S. Chen, T. Zhou, Q. Du, D. Wang, A. Gilardi, J. L. Vay, D. Li, J. van Tilborg, C. Schroeder, E. Esarey, R. Wilcox, and C. Geddes, "Broadband spectral combining of three pulse-shaped fiber amplifiers with 42fs compressed pulse duration," Opt. Express 31, 12717-12724 (2023). DOI: https://doi.org/10.1364/OE.486884.
- 22. L. A. Siiman, W. Z. Chang, T. Zhou, and A. Galvanauskas, "Coherent femtosecond pulse combining of multiple parallel chirped pulse fiber amplifiers," Opt. Express 20, 18097-18116 (2012). DOI: https://doi.org/10.1364/OE.20.018097.
- 23. V. W. S. Staels, E. C. Jarque, D. Carlson, M. Hemmer, H. C. Kapteyn, M. M. Murnane, and J. S. Roman, "Numerical investigation of gas-filled multipass cells in the enhanced dispersion regime for clean spectral broadening and pulse compression," Opt. Express 31, 18898-18906 (2023). DOI: https://doi.org/10.1364/OE.481054.
- 24. S. J. Wang, B. W. Liu, C. L. Gu, Y. J. Song, C. Qian, M. L. Hu, L. Chai, and C. Y. Wang, "Self-similar evolution in a short fiber amplifier through nonlinear pulse preshaping," Opt Lett 38, 296-298 (2013). DOI: https://doi.org/10.1364/Ol.38.000296.

25. T. M. Shay, V. Benham, J. T. Baker, A. D. Sanchez, D. Pilkington, and C. A. Lu, "Self-synchronous and self-referenced coherent beam combination for large optical arrays," Ieee. J. Sel. Top. Quant 13, 480-486 (2007). DOI: https://doi.org/10.1109/Jstqe.2007.897173.